

## Invited

## The Multiple-Tunnel Junction (MTJ) and its Application to Single-Electron Memory and Logic

K. Nakazato and \* H. Ahmed

Hitachi Cambridge Laboratory, Cavendish Laboratory,  
Madingley Road, Cambridge, CB3 0HE, U.K.

\* Microelectronics Research Centre, Cavendish Laboratory,  
Madingley Road, Cambridge, CB3 0HE, U.K.

The multiple-tunnel junction (MTJ) by making a side-gated constriction in  $\delta$ -doped GaAs is demonstrated as a basic component of single-electronics. A single-electron memory cell, in which one bit of information is represented by the excess or shortfall of a precise number of electrons, was fabricated and the operation was confirmed at liquid helium temperatures. A new switching element, the variable-barrier MTJ, and a new circuit, the single-charge injection logic circuit, are proposed.

### 1. Introduction

Modern nano-technology enables us to fabricate very small structures with capacitance small enough to observe the charging effects of discrete electrons. When the charging energy  $e^2/2C$  of the island capacitance  $C$  becomes larger than the energy  $k_B T$  of the thermal fluctuations, the entrance of one electron results in a noticeable recharging of the island capacitance, so that electron transfer is strongly suppressed. Based on this Coulomb blockade effect, several new devices have been proposed and demonstrated <sup>1,2</sup>. The important applications are in the single-electron memory and in logic circuits, which are characterised by their low power consumption.

### 2. Multiple-Tunnel Junction

One of the most important elements for utilising charging effects is the Multiple-Tunnel Junction (MTJ) in which a series of small islands is formed. The charging energy of the island creates an energy barrier which blocks the entrance of electrons into the MTJ so that multi-stable states of different numbers of electrons can be formed. The MTJ is also important in suppressing offset-charge and co-tunnelling effects.

A number of different techniques have been employed to realise ultra-small tunnel junctions, including double-angle evaporation of Al and Schottky gate confinement of the two-dimensional electron gas (2DEG) formed at the GaAs/AlGaAs heterointerfaces. These methods provide only a single tunnel junction and the overall size becomes large when a MTJ is constructed by connecting these elements. To realise very small MTJ structures, we have used a side-gated structure in  $\delta$ -doped GaAs <sup>3</sup>. The  $\delta$ -doped layers are suitable for miniaturisation because of the small depletion lengths resulting from the high carrier concentration and the

relatively shallow depth of the 2DEG. Furthermore, large potential fluctuations ( $\sim 30$  meV) in the  $\delta$ -doped layer create several small islands in a constriction without the need for lithography to define the individual islands.

The  $\delta$ -doped GaAs wafer was grown by Metalorganic Chemical Vapour Deposition (MOCVD). The electron channel formed in the  $\delta$ -doped layer is situated 30 nm below the GaAs surface and is a few atomic layers in thickness. It is doped with Si to a concentration of  $5 \times 10^{12}$  cm<sup>-2</sup>. An MTJ was formed by an etched constriction with a width of 150 nm and length of 400 nm as shown in Fig. 1 (a). The Fermi energy of the electrons in the constriction can be modified by biasing the side-gate.

Current-voltage characteristics were measured using standard equipment as shown in Fig. 2. The observed Coulomb-blockade oscillations were explained by postulating a series of microsegments split by donor atom potentials and forming a series of single-electron transistors <sup>3</sup>. The formation of several islands is supported by another measurement in the highly pinched-off region of operation in that negative resistances due to resonant tunnelling among microsegments have been observed, and by the calculation of conductance modelled using standard single-particle recursive Green's function techniques <sup>4</sup>. The calculated potential landscape is shown in Fig. 1 (b). There are large potential fluctuations within the channel, and more than five potential wells are evident for the random impurity configuration used for this simulation.

### 3. Single-Electron Memory

A direct application of MTJs is the single-electron memory in which one bit of information can be represented by the excess or shortfall of a precise number of electrons <sup>5</sup>. The principal parts of a single-electron memory cell consist of a gate-capacitor and a MTJ as

shown in Fig. 3 (a). The memory node voltage  $V$  depends both on the voltage  $V_g$  applied to the gate and on the charge stored on the node,

$$V = \frac{e}{C_\Sigma} \left( \frac{C_g V_g}{e} - n \right) \quad (1)$$

Here  $n$  is the number of excess electrons on the memory node and  $C_\Sigma$  is the total capacitance  $C + C_g + C_s$ , where  $C$  is the capacitance of the MTJ,  $C_g$  is the gate capacitance, and  $C_s$  is the stray capacitance. Equation (1) is plotted in Fig. 3 (b) where cyclic operation of gate voltage is assumed. Within a Coulomb blockade regime electrons cannot enter or exit the memory node. When  $V$  reaches the boundary of this Coulomb blockade regime, one electron enters or leaves to keep the electron state inside the Coulomb blockade regime. By applying a gate-voltage pulse  $V_g$  with magnitude larger than  $eC_\Sigma/(CC_g)$ , the number of electrons on the memory node can be changed. In Fig. 3 (b) the lower branch corresponds to a stable state with an excess of two electrons, and the upper branch to a stable state with a shortfall of two electrons from the charge neutrality state. In general, one bit of information can be represented by  $+N$  and  $-N$  electron number states, where  $N$  is given by the integer part of  $C_\Sigma/2C$ .

The experimental single-electron memory device consists of three MTJs and two capacitors as shown in Fig. 4. MTJ1 controls single-electron transfer to the memory node. MTJ2 is used to characterise MTJ1; the side-gate voltage dependence on the conductance of MTJ1 is measured by opening MTJ2. When memory characteristics are measured, MTJ2 is pinched off by applying a large negative voltage to the side-gate. MTJ3 is used as an electrometer to detect the memory node voltage.

The experimental circuit shows single-electron characteristics as a function of side-gate voltages (Fig. 5). Nano-ampere current levels are measured at higher side-gate voltages at a drain voltage of 1 mV. Turnstile current is observed at an intermediate side-gate voltage region when ac (10MHz) gate voltage is applied. At lower side-gate voltages single-electron memory effects are observed. At even lower side-gate voltages an insulating-state appears.

The memory cell characteristic is shown in Fig. 6. Clear and reproducible hysteresis is observed. From the estimation of capacitance,  $C = 5$  aF,  $C_g = 200$  aF, and  $C_s = 200$  aF, the upper and the lower branches correspond to  $\pm 40$  electrons. The hysteresis predicted in Fig. 3 is quite universal, independent of not only the absolute value of the gate voltage but also the gate voltage range. These universal characteristics are clearly observed for several gate voltage ranges.

From the orthodox theory<sup>1,2)</sup>, the area of the hysteresis loop  $A_h$  depends on temperature  $T$  and sweep rate  $v_s$  of gate voltage as follows;

$$A_h = A_{h0} \left\{ 1 + a \left( Ck_B T / e^2 \right) \ln \left( v_s C_g N_t C R / e \right) \right\} \quad (2)$$

where  $A_{h0}$  is the area of the hysteresis loop at zero temperature,  $R$  is the total resistance of the MTJ, and  $a$  is a constant around 10. Experiments<sup>5)</sup> show the clear

dependence on temperature and gate-voltage sweep-rate as predicted in eq. (2), and the hysteresis is determined by intrinsic memory effects, not by co-tunneling effects as previously reported<sup>6)</sup>. One of the reasons that intrinsic memory effects are observed in our sample is that the tunnel resistance can be modified in our structures by biasing the side-gate and can be tuned to the point where co-tunneling is reduced significantly<sup>7)</sup>.

#### 4. Single-Electron Logic

A switching element based on a variable-barrier MTJ is proposed, in which the 'ON' state is represented by a Bloch state with tunnel resistance less than the quantum resistance, and an 'OFF' state is represented by the Coulomb blockade state with tunnel resistance larger than the quantum resistance. The Coulomb gap voltage is schematically shown as a function of tunnel barrier voltage in Fig. 7 (a), which gives an ideal transfer characteristic of the inverter circuit.

Using such variable-barrier MTJs, a new circuit scheme, the single-charge injection logic, is proposed as shown in Fig. 7 (b). In this scheme a voltage pulse is applied instead of constant voltage to refresh output information; single-charges are injected to the output node and the number of electrons is settled according to the Coulomb gap voltage of the MTJs. When the capacitance of the output node is reduced, the number of electrons needed to represent the information becomes small but stable operation can still be realised due to the charge quantisation on the output node. The merits of this circuit are (1) insensitivity to offset-charges and co-tunneling, (2) sufficient voltage gain, (3) ideal non-linear characteristics for information recovery, (4) almost independence from device parameters, (5) any electron number can represent one bit of information.

#### References

- 1) D. V. Averin and K. K. Likharev, in "Mesoscopic Phenomena in Solids," ed. by B. L. Altshuler, P. A. Lee, and R. A. Webb (North-Holland, Amsterdam, 1991), p. 173.
- 2) H. Grabert and M. H. Devoret, ed., "Single Charge Tunneling," (Plenum, New York, 1992).
- 3) K. Nakazato, T. J. Thornton, J. White, and H. Ahmed, Appl. Phys. Lett. **61**, 3145 (1992).
- 4) R. J. Blaikie, K. Nakazato, R. B. S. Oakeshott, J. R. A. Cleaver, and H. Ahmed, Appl. Phys. Lett. **64**, 118 (1994).
- 5) K. Nakazato, R. J. Blaikie, J. R. A. Cleaver, and H. Ahmed, Electron. Lett. **29**, 384 (1993). K. Nakazato, R. J. Blaikie, and H. Ahmed, J. Appl. Phys. **75**, 5123 (1994).
- 6) T. A. Fulton, P. L. Gammel, and L. N. Dunkleberger, Phys. Rev. Lett. **67**, 3148 (1991). P. Lafarge, P. Joyez, H. Pothier, A. Cleland, T. Holst, D. Esteve, C. Urbina, and M. H. Devoret, C. R. Acad. Sci. Paris, **314**, Ser. II, 883 (1992).
- 7) Y. Nagamine, H. Sakaki, L. P. Kouwenhoven, L. C. Mur, C. J. P. M. Harmans, J. Motohita, and H. Noge, Appl. Phys. Lett. **64**, 2379 (1994).
- 8) K. Yano, T. Ishii, T. Hashimoto, T. Kobayashi, F. Murai, and K. Seki, Tech. Digest of IEDM93, 541 (1993).

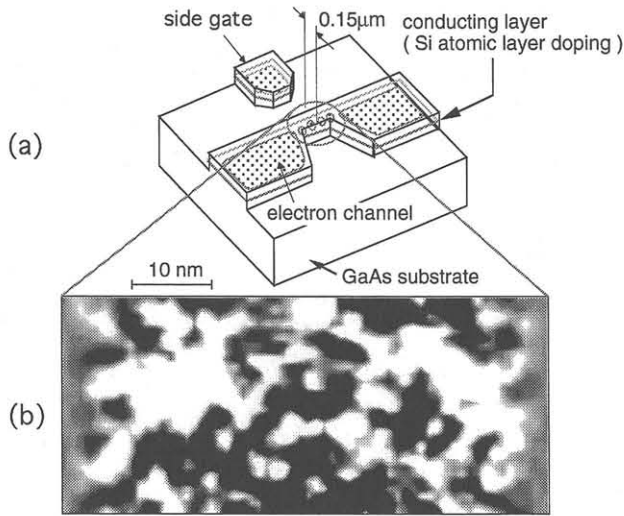


Fig.1 (a) MTJ using a side-gated structure in  $\delta$ -doped GaAs. (b) Calculated electron channel.

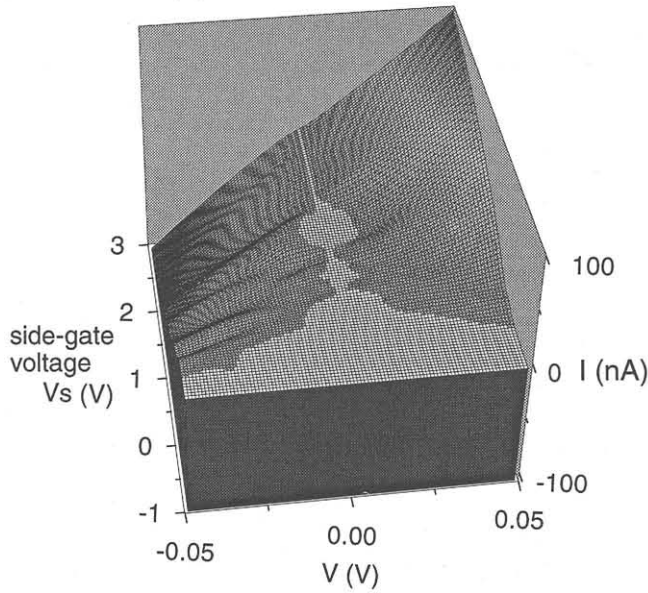


Fig.2 I-V characteristic at 1.3K.

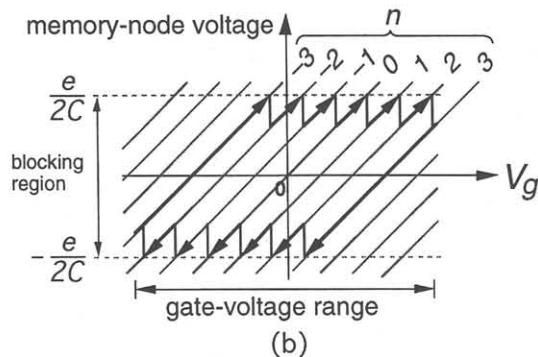
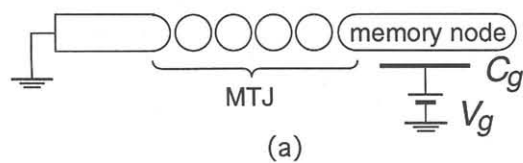


Fig.3 (a) Principal part of single-electron memory. (b) Principle of operation.

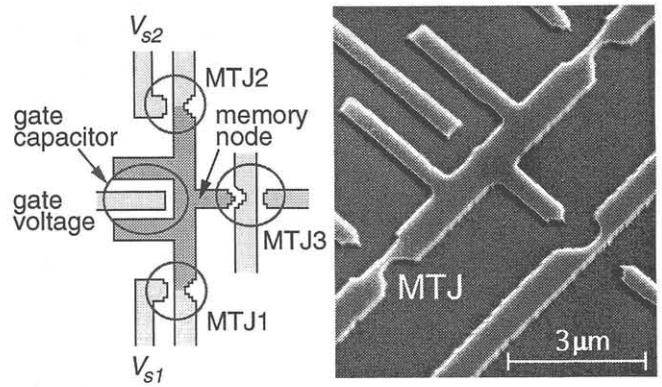


Fig.4 Scanning electron micrograph of an experimental single-electron memory device.

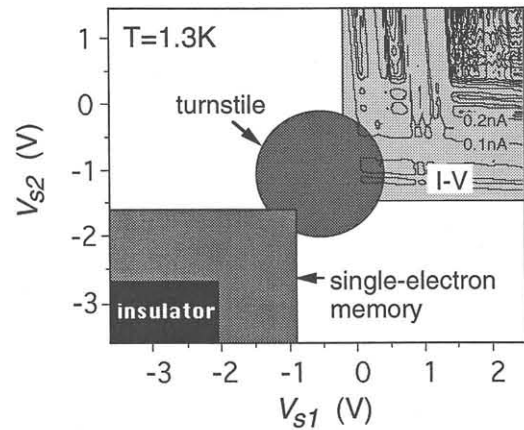


Fig.5 Operation region of some single-electron effects.

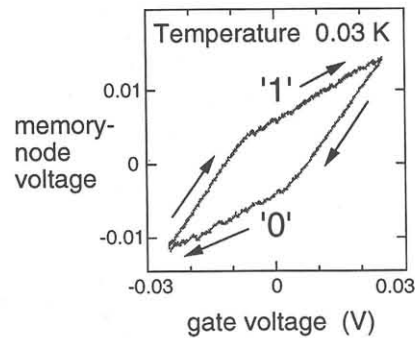


Fig.6 Memory operation characteristic.

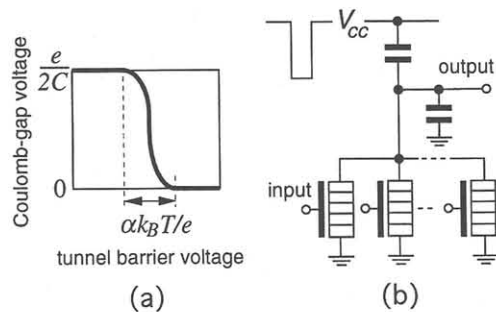


Fig.7 (a) Coulomb-gap voltage of a variable-barrier MTJ. (b) Single-charge injection logic.